

# Effects of Frequency and Bias Voltage on Dielectric Properties and Electric Modulus of Au/Bi<sub>4</sub>Ti<sub>3</sub>O<sub>12</sub>/n-Si (MFS) Capacitors

*Araştırma Makalesi / Research Article*

Perihan DURMUŞ<sup>1,\*</sup>, Çiğdem BİLKAN<sup>1</sup>, Mert YILDIRIM<sup>2</sup>

<sup>1</sup>Department of Physics, Gazi University, 06500, Ankara, Turkey

<sup>2</sup>Department of Mechatronics Engineering, Düzce University, 81620, Düzce, Turkey

(Geliş/Received : 18.11.2016 ; Kabul/Accepted : 05.01.2017 )

## ABSTRACT

In this work, a metal-ferroelectric-semiconductor (MFS) type capacitor was fabricated and admittance measurements were held in a wide frequency range of 1 kHz-5 MHz at room temperature for the investigation of frequency and voltage dependence of complex dielectric constant, complex electric modulus and electrical conductivity of the MFS capacitor. Bismuth titanate (Bi<sub>4</sub>Ti<sub>3</sub>O<sub>12</sub>) with high dielectric constant was used as interfacial ferroelectric material and the structure of MFS capacitor was obtained as Au/Bi<sub>4</sub>Ti<sub>3</sub>O<sub>12</sub>/n-Si. Experimental results showed that dielectric, modulus and conductivity parameters are strong functions of frequency and voltage especially in depletion and accumulation regions due to the existence of surface states (N<sub>ss</sub>), series resistance (R<sub>s</sub>), interfacial polarization and interfacial layer. It was found that R<sub>s</sub> of the structure and interfacial ferroelectric layer are effective in accumulation region whereas surface states (N<sub>ss</sub>) and interfacial polarization are effective in depletion region. Also the changes in dielectric, modulus and conductivity parameters become considerably high particularly at low frequencies due to high values of R<sub>s</sub> and N<sub>ss</sub>. The observed anomalous peak in voltage dependent plots of capacitance and dielectric constant was attributed to the particular density distribution of N<sub>ss</sub>, R<sub>s</sub> and minority carrier injection. Moreover, the value of conductivity at low and intermediate frequencies is almost independent of frequency thus low frequency data was used to extract d.c. conductivity. This work showed that the use of high-dielectric Bi<sub>4</sub>Ti<sub>3</sub>O<sub>12</sub> as ferroelectric interfacial layer in a MFS capacitor is preferable due to high values of its dielectric constant compared with traditional insulator layer materials such as SiO<sub>2</sub> and SnO<sub>2</sub>. Therefore, a MFS capacitor with Bi<sub>4</sub>Ti<sub>3</sub>O<sub>12</sub> interfacial layer can store more energy thanks to its high dielectric constant.

**Keywords:** MFS capacitors, frequency and voltage dependence, surface states and interfacial polarization, dielectric properties and electrical modulus.

## 1. INTRODUCTION

Electrical and dielectric properties of metal-semiconductor (MS) type structures with an insulator, polymer and ferroelectric interlayers are usually different from the ideal case of conventional MS structures especially due to barrier inhomogeneity and variations in the energy dependent surface states (N<sub>ss</sub>) and concentration of doping atoms as a result of growing interlayer. Therefore, there has been a great effort for enhancing the performance metal-semiconductor (MS) structures by using interfacial materials with high dielectric constant such as TiO<sub>2</sub> [1-3] Bi<sub>3</sub>Ti<sub>4</sub>O<sub>12</sub> (BTO) [4,5], BaTiO<sub>3</sub> [6], (graphene-oxide-doped PrBaCoO nanoceramics) [7], (7% graphene doped-PVA) [8] and (Al<sub>2</sub>O<sub>3</sub>/Ga<sub>2</sub>O<sub>3</sub>(Gd<sub>2</sub>O<sub>3</sub>)) [9]. Among these various interlayer materials, ferroelectrics come forward since not only it provides high dielectric constant but also it is suitable for photodiode and non-volatile memory applications [10]. These device applications mostly utilize metal-ferroelectric-semiconductor (MFS) structures therefore the study of metal-ferroelectric-semiconductor (MFS) structures is important. During admittance measurements, MFS structures behave like a series combination of typical parallel plate capacitors in

the high frequency limit. Therefore, charge storage ability of the capacitor also depends on the dielectric constant of the ferroelectric material. Therefore, the capacitance is given by  $\epsilon'\epsilon_0 A/d$  where  $\epsilon'$  is dielectric constant,  $\epsilon_0$  is permittivity of vacuum, A is capacitor area and d is the thickness of interfacial layer. Modifying the capacitance through changing the values of A and d is limited due to high space coverage and operating voltage in electronic devices [9,11], on the other hand charge storage ability of the capacitor is enhanced by using materials with high dielectric constant. It must also be noted that surface states (N<sub>ss</sub>) with energies that correspond to forbidden band gap are formed in a way that they are in equilibrium with the semiconductor [12-15]. Nevertheless, the effect of N<sub>ss</sub> is minimized by performing the admittance measurements at high frequencies.

When the thickness of interfacial ferroelectric layer is small, the device behaves like a typical Schottky barrier diode which could be utilized as photodiode, solar cell, and alike. However, when the thickness is sufficiently large, it becomes difficult for the charges on metal and semiconductor to exchange, hence the charge storage feature of the MFS structure comes forward, and therefore MFS structure basically behaves like a MFS capacitor which could be utilized in ferroelectric field effect transistors [16-19]. Like the other kinds of MS structures with various interlayer materials, the

\*Sorumlu Yazar (Corresponding Author)  
e-posta : pdurmuz@gazi.edu.tr

performance and reliability of a MFS structure are dependent of various factors/parameters such as the interfacial layer thickness, its homogeneity and dielectric constant, the process of surface preparation or fabrication processes, doping concentration of donor or acceptor atoms ( $N_D$  or  $N_A$ ), barrier formation at M/S interface and its homogeneity, density of  $N_{ss}$  or dislocations at interlayer/semiconductor interface, series resistance ( $R_s$ ) of device, as well as measurement conditions such frequency of a.c. signal, applied bias voltage and device temperature [20-24].

The aim of this study is to investigate the effects of frequency and applied bias voltage on the dielectric properties, electric modulus and electrical conductivity of Au/Bi<sub>4</sub>Ti<sub>3</sub>O<sub>12</sub>/n-Si (MFS) capacitors. For this purpose, admittance measurements were carried out in wide frequency (1 kHz-5 MHz) and bias voltage ( $\pm 4$ V) ranges at room temperature. Obtained capacitance (C) and conductance (G) data were utilized for calculating dielectric, electric modulus and electrical conductivity parameters. Dependence of these parameters on frequency and bias voltage was clear. The bias voltage dependence was explained by the effects of  $R_s$ ,  $N_{ss}$  and interfacial BTO layer whereas the frequency dependence was explained by Maxwell-Wagner polarization.

## 2. EXPERIMENTAL DETAILS

Au/Bi<sub>4</sub>Ti<sub>3</sub>O<sub>12</sub>/n-Si (MFS) capacitor was fabricated using phosphor doped single crystal Si wafer with diameter of 3 inches, orientation of (111) and thickness of  $\sim 300$   $\mu$ m. Before the fabrication, n-Si wafer was cleaned in a mixture of a peroxide-ammoniac solution and then in H<sub>2</sub>O+HCl solution for 10 min and then it was thoroughly rinsed in deionized-water with 18 M $\Omega$  cm resistivity in an using an ultrasonic bath for 15 minutes. After the cleaning process, the wafer was immediately taken into thermal evaporator in which highly pure (99.999%) Au metal was evaporated onto the whole back side of n-Si wafer at  $10^{-6}$  Torr. Thus, 200 nm gold layer was grown on the wafer. However it needed to be annealed at 450  $^{\circ}$ C for 5 min in N<sub>2</sub> atmosphere to get an ohmic contact with low resistivity by sintering the Au layer. After the formation of ohmic contact, Bi<sub>4</sub>Ti<sub>3</sub>O<sub>12</sub> ferroelectric interfacial layer was deposited on the front side of n-Si wafer by RF magnetron sputtering using a hot

compacting of Bi<sub>4</sub>Ti<sub>3</sub>O<sub>12</sub> powder of a stoichiometric composition as a target material. The mixture of argon (Ar) and oxygen (O<sub>2</sub>) was used as working medium and the substrate was kept at 650  $^{\circ}$ C. Thickness of the deposited BTO layer was measured with Veeco Dektak 6 M thickness profilometer as 540 nm. Finally, circle-shaped pure Au (99.999%) front contacts with diameter of 1 mm were deposited through same thermal evaporation system and conditions. Thus, 200 nm gold layer was grown on BTO layer so that the fabrication of MFS capacitor is completed. In order to perform admittance measurements, the fabricated Au/Bi<sub>4</sub>Ti<sub>3</sub>O<sub>12</sub>/n-Si (MFS) capacitor was mounted on a copper holder with the help of silver dag and later the electrical contact with one of the front contacts was ensured by the use of thin silver coated Cu wires with the help of silver paste. C-V-f and G/ $\omega$ -V-f data was obtained by using a HP4192A LF impedance analyzer between  $-4$  V and  $+4$  V at room temperature. During the measurements, the MFS capacitor was applied with a small a.c. test signal of 40 mV<sub>rms</sub> in a wide frequency range of 1 kHz and 5 MHz. All measurements were carried out with the help of a microcomputer through an IEEE-488 ac/dc converter card.

## 3. RESULT AND DISCUSSION

Admittance spectroscopy has proven to be an efficient tool for characterizing electrical parameters such as traps, series resistance, doping concentration, barrier height, depletion width and dielectric parameters of Schottky barrier diodes (SBDs) and capacitors of the similar heterostructure. For this purpose, admittance measurements were held in a wide frequency and/or temperature range. Figure 1 (a) and (b) show C-V and G/ $\omega$ -V plots of Au/Bi<sub>4</sub>Ti<sub>3</sub>O<sub>12</sub>/n-Si capacitor, respectively.

These plots clearly exhibit inversion, depletion and accumulation regions just like a typical SBD. There is a peak behavior just after the depletion region for C-V curves at low frequencies and then the capacitance value drops rapidly particularly for the data measured at 1 kHz. Such peak behavior is common for the structures that has interfacial layer of insulator type. On the other hand, the decrease after the peak is stronger at low frequencies because of  $R_s$  of the capacitor. Another reason of peak

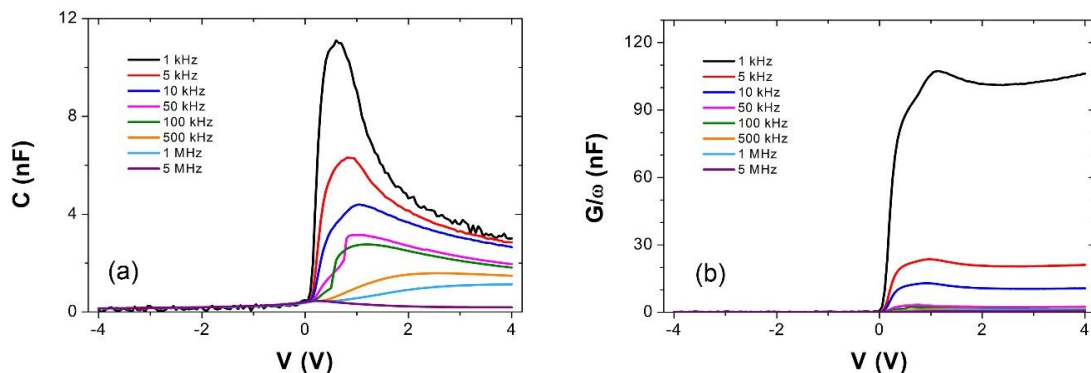


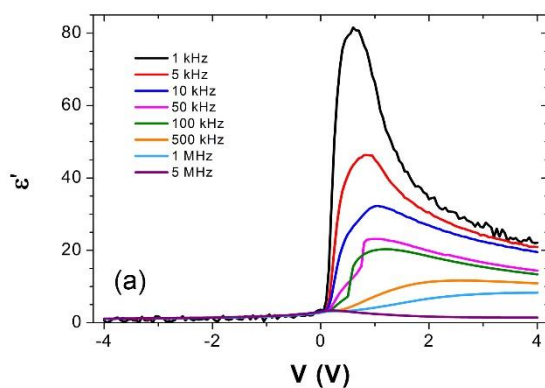
Figure 1. (a) C-V and (b) G/ $\omega$ -V plots of the MFS capacitor at different frequencies.

behavior at low frequencies is due to the effect of  $N_{ss}$  because excess capacitance and conductance is yielded for admittance data measured at low frequencies. This effect also shows itself in  $G/\omega$ - $V$  plots such that higher conductance values are obtained at low frequencies due to the contribution of excess conductance formed by  $N_{ss}$ . The effects of  $R_s$  and  $N_{ss}$  on capacitance and conductance is important since dielectric parameters are calculated using the measured capacitance and conductance values. This is also because the applied bias on the semiconductor device is shared by  $R_s$ ,  $N_{ss}$  and interfacial layer. However, while the value of  $R_s$  on the C-V and  $G/w$ -V is effective only the accumulation region, surface states ( $N_{ss}$ ) are effective both in inversion and depletion regions. When the life time of surface states is lower than the period ( $T$ ), the charges at surface states can easily follow the external ac signal and yield an excess capacitance and conductance to their measured value. Therefore, this effect becomes more effective in the low and intermediate frequency regions ( $T=1/f$ ) and at enough high frequencies ( $f \geq 500$  kHz) the effect of  $N_{ss}$  can be neglected low. Because, the life time of surface states ( $\tau$ ) at high frequencies becomes higher than  $T$ . Nicollian and Brew suggested that real part of impedance in the high accumulation region yields  $R_s$ , thus  $R_s$  values were calculated using the equation below [21];

$$R_s = \frac{G}{G^2 + \omega^2 C^2}$$

In addition, Fonash's method [25] was utilized for the calculation of  $N_{ss}$  values which can be calculated by the following equation;

$$\alpha = \frac{qdN_{ss}}{\epsilon_i}$$



increasing frequency. As the frequency of a.c. signal is increased, period of the signal gets smaller and after some point it becomes smaller than the time constant of interface states. Therefore, interface states cannot follow the a.c. signal and contribution of excess capacitance is minimized.  $R_s$  values also decrease with increasing frequency in consistency with the increasing conductance values with increasing frequency.

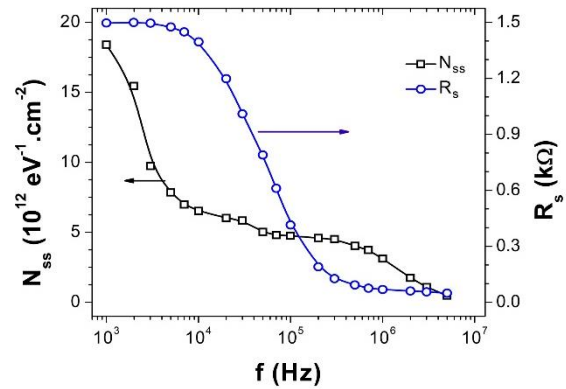


Figure 2. Frequency dependence of  $N_{ss}$  and  $R_s$  of the MFS capacitor.

It is well known that permittivity ( $\epsilon^*$ ) consists of real and imaginary parts such that it is equal to  $\epsilon' - i\epsilon''$  where  $\epsilon'$  is a measure of the capacitor's ability to store charge and  $\epsilon''$  is associated with the energy dissipation, and they are referred as dielectric constant and dielectric loss, respectively. These parameters are calculated on the basis that fabricated MFS device is literally a combination of parallel plate capacitor, thus dielectric constant and dielectric loss are obtained by using the following equations [1,2,3,5,7,8];

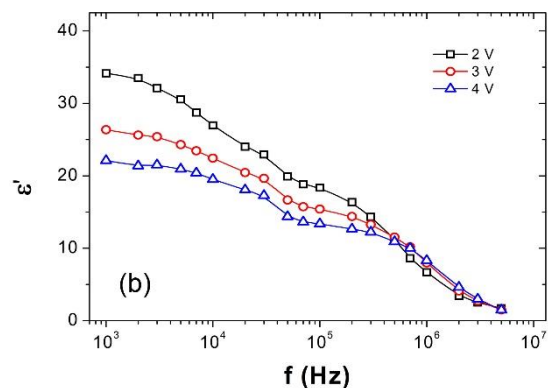


Figure 3. (a)  $\epsilon'$ - $V$  and (b)  $\epsilon'$ - $f$  plots of the MFS capacitor.

where  $\epsilon_i$  is dielectric constant of insulating BTO layer,  $q$  is electronic charge,  $d$  is the thickness of insulating BTO layer and  $\alpha$  is a parameter given by  $(1-c_2)/c_2$  where  $c_2$  corresponds to the ratio of experimental value of doping concentration to its theoretical value ( $7,837 \times 10^{16} \text{ cm}^{-3}$ ) such that the experimental value can be extracted from the slope of  $C^2$ - $V$  curves [4]. Figure 2 shows frequency dependence of  $N_{ss}$  and  $R_s$  of Au/ $\text{Bi}_4\text{Ti}_3\text{O}_{12}$ /n-Si capacitor. As previously discussed,  $N_{ss}$  values decrease with

$$\epsilon' = \frac{C}{C_o}$$

$$\epsilon'' = \frac{G}{\omega C_o}$$

Here  $C_o$  is the capacitance of empty capacitor and equals to  $\epsilon_o A/d$  where  $\epsilon_o$  is permittivity of vacuum ( $8.85 \times 10^{-14} \text{ F/cm}$ ) and  $A$  is the area of front contact. Bias voltage and

frequency dependent plots of dielectric constant of Au/Bi<sub>4</sub>Ti<sub>3</sub>O<sub>12</sub>/n-Si (MFS) capacitor is given in Figure 3 (a) and (b) respectively. Similarly, bias voltage and frequency dependent plots of dielectric loss of the MFS capacitor are given in Figure 4 (a) and (b), respectively.

that the latter is reciprocal of the former, i.e.  $M^* = 1/\epsilon^*$  [1,2,3,5,7,8], therefore real and imaginary parts of electric modulus are calculated using the following equation;

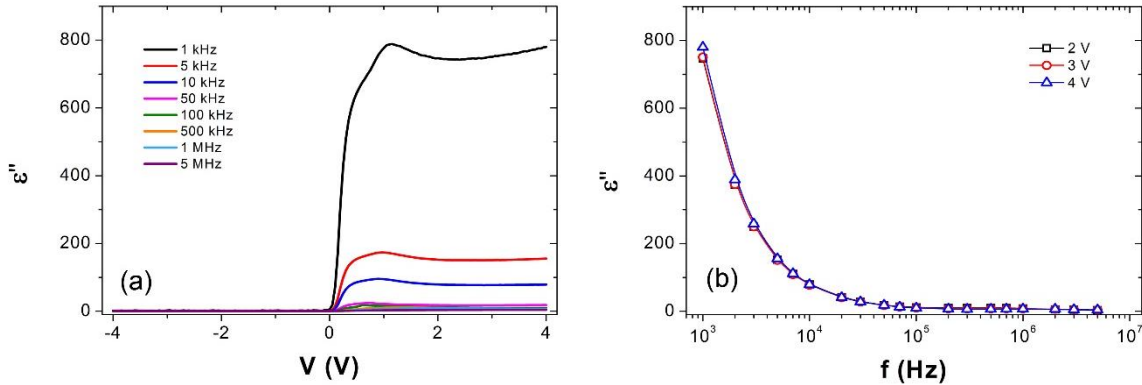


Figure 4. (a)  $\epsilon''$ -V and (b)  $\epsilon''$ -f plots of the MFS capacitor.

Voltage dependence of these dielectric parameters resembles to that of admittance data. Therefore similar peak behavior is observed at low frequencies due to high values of  $R_s$  and  $N_{ss}$ . In Figure 3 (b) and Figure 4 (b), it is clear that  $\epsilon'$  and  $\epsilon''$  decrease with increasing frequency.  $\epsilon'$  also shows strength of polarization in the studied material. It is well known that polarization is comprised of interfacial polarization, dipolar polarization, ionic polarization and electronic polarization. Last three polarization types exist in the whole frequency range of a.c. signal of applied to the MFS capacitor. However, contribution of interfacial polarization, which is also called as Maxwell-Wagner polarization, to total polarization disappears as the frequency goes up to MHz level. Therefore, we observe a gradual decrease in  $\epsilon'$  values with increasing frequency. On the other hand, there is a rapid decrease for  $\epsilon''$  values with no sign of relaxation. Nevertheless, it might be masked due to conductivity of the MFS capacitor, hence dielectric properties of Au/Bi<sub>4</sub>Ti<sub>3</sub>O<sub>12</sub>/n-Si (MFS) capacitor are further explored using electric modulus ( $M^*$ ) approach. The relation between permittivity and electric modulus is

$$M^* = M' + iM'' = \frac{\epsilon'}{\epsilon'^2 + \epsilon''^2} + i \frac{\epsilon''}{\epsilon'^2 + \epsilon''^2}$$

Figure 5 (a) and (b) show bias voltage and frequency dependent plots of  $M'$ , and same plots of  $M''$  are shown in Figure 6 (a) and (b), respectively. The reciprocal behavior of modulus plots is particularly clear for the frequency dependent plots. The increase in these parameters with increasing frequency is already expected for this reason. Besides,  $M''$ -f plots reveal peaks as can be seen in inset of Figure 6 (b). Such peak behavior of  $M''$  data is associated with the relaxation of the sample. Therefore, it can be said that relaxation frequency of the sample is around 70 kHz.

When the MFS capacitor is applied with a.c. signal, its electrical conductivity is referred as a.c. conductivity ( $\sigma_{ac}$ ). The values of  $\sigma_{ac}$  were calculated using the equation  $\sigma_{ac} = \omega \epsilon'' \epsilon_0$  [1,2,3,5,7,8] and its bias voltage dependence is given in Figure 7 (a). The MFS capacitor yields much larger conductivity values in the forward bias region compared to reverse bias region because the MFS

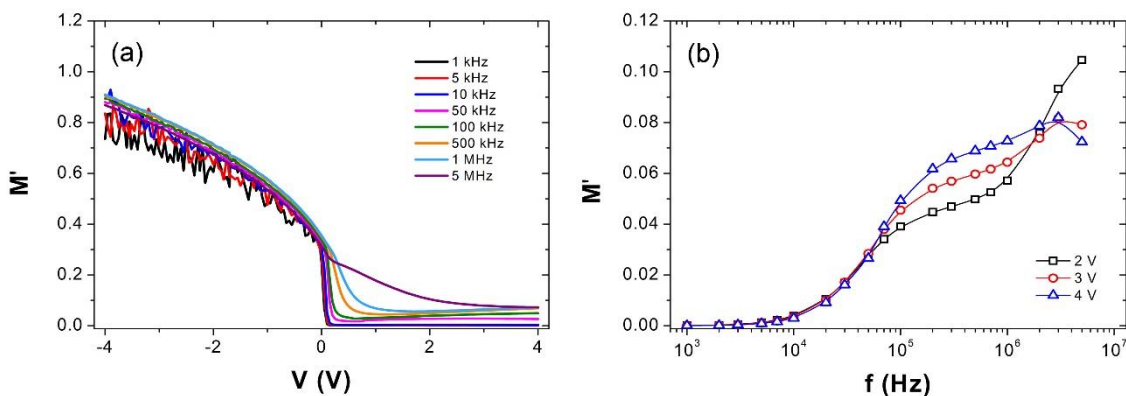


Figure 5. (a)  $M'$ -V and (b)  $M'$ -f plots of the MFS capacitor.

capacitor is in the form of a Schottky barrier diode. Figure 7 (b) shows frequency dependence of  $\sigma_{ac}$ .

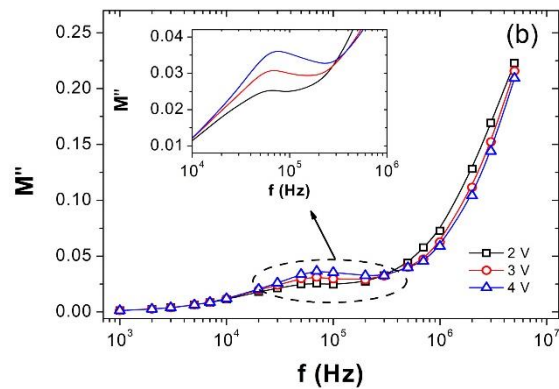
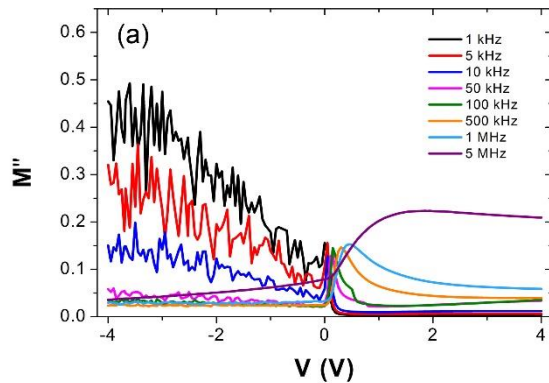


Figure 6. (a)  $M''$ - $V$  and (b)  $M''$ - $f$  plots of the MFS capacitor.

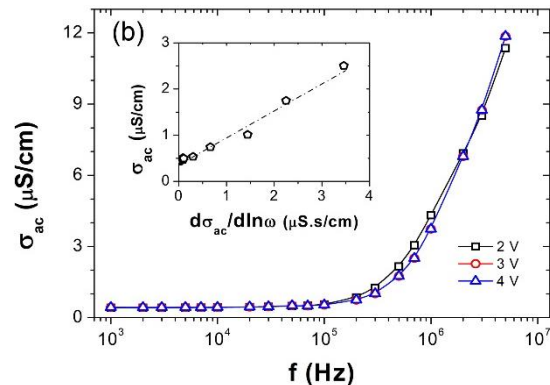
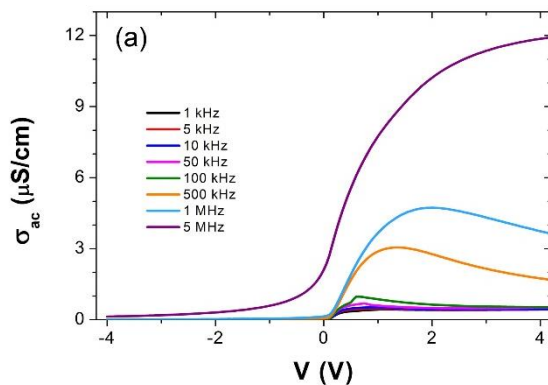


Figure 7. (a)  $\sigma_{ac}$ - $V$  and (b)  $\sigma_{ac}$ - $f$  plots of the MFS capacitor. The inset shows the  $\sigma_{ac} - d\sigma_{ac}/d\ln\omega$  plot.

It is seen that  $\sigma_{ac}$ - $f$  plots increase gradually up to 0.1 MHz, then they increase rapidly. The increase in  $\sigma_{ac}$  with increasing frequency leads to an increase in eddy current and this is consistent with the decreasing strength of series resistance with frequency (Figure 2).  $\sigma_{ac}$  is a combination of capacitor's d.c. conductivity ( $\sigma_{dc}$ ) and conductivity contribution due to a.c. signal, and its frequency dependence is expressed by the following equation [1,2,3,5,7,8];

$$\sigma_{ac} = \sigma_{dc} + A\omega^s$$

where  $A$  is a constant and  $s$  is a parameter that shows the strength of frequency dependence. Another expression of frequency dependence of  $\sigma_{ac}$  is as below [5];

$$\sigma_{ac} = \sigma_{dc} + \frac{1}{s} \frac{d\sigma_{ac}}{d \ln \omega}$$

Inset of Figure 7 (b) shows  $\sigma_{ac} - d\sigma_{ac}/d \ln \omega$  plot whose y-intercept corresponds to  $\sigma_{dc}$ . Thus,  $\sigma_{dc}$  of the MFS capacitor was extracted as  $4.1 \times 10^{-7}$  S/cm. This value might look small, however it is reasonable considering the thickness of BTO interlayer.

#### 4. CONCLUSION

The fabricated Au/Bi<sub>4</sub>Ti<sub>3</sub>O<sub>12</sub>/n-Si MFS capacitor yielded high values of capacitance and conductance particularly

at low frequencies. This was explained by the excess capacitance and conductance due to interface states.

Interface states and series resistance were the reasons of peak behavior in C-V and G/ $\omega$ -V plots. When these two parameters were calculated, it was seen that they decrease with increasing frequency. Similar effect was also seen in dielectric constant and dielectric loss such that they decrease as the frequency is increased because interface states can no longer follow a.c. signal since lifetime of traps is larger than inverse of angular frequency. Dielectric constant at 1 kHz is around 20s in the high accumulation region. Modulus formalism was utilized to explore relaxation behavior of the capacitor and it was found that relaxation occurs around ~70 kHz. Moreover, investigation of a.c. conductivity in the low frequency region revealed a d.c. conductivity value of  $4.1 \times 10^{-7}$  S/cm. Overall, the usage of BTO interfacial layer is preferable due to high value of dielectric constant because it allows storing more energy and enhance capacitor's ability.

#### REFERENCES

- [1] Asar Y. Ş., Asar T., Altındal Ş. and Özçelik S., "Dielectric spectroscopy studies and ac electrical conductivity on (AuZn)/TiO<sub>2</sub>/p-GaAs (110) MIS structures", *Philosophical Magazine*, 95: 2885-2898, (2015).
- [2] Asar Y. Ş., Asar T., Altındal Ş. and Özçelik S., "Investigation of dielectric relaxation and ac electrical conductivity using impedance spectroscopy method in

- (AuZn)/TiO<sub>2</sub>/p-GaAs (110) schottky barrier diodes” *Journal of Alloys and Compounds*, 628: 442-449, (2015).
- [3] Tanrikulu E. E., Yıldız D. E., Günen A. and Altındal Ş., “Frequency and voltage dependence of electric and dielectric properties of Au/TiO<sub>2</sub>/n-4H-SiC (metal-insulator-semiconductor) type Schottky barrier diodes”, *Physica Scripta*, 90: 095801, (2015).
- [4] Yıldırım M., Durmuş P. and Altındal Ş., “Analyses of temperature-dependent interface states, series resistances, and AC electrical conductivities of Al/p-Si and Al/Bi<sub>4</sub>Ti<sub>3</sub>O<sub>12</sub>/p-Si structures by using the admittance spectroscopy method”, *Chinese Physics B*, 22: 108502, (2013).
- [5] Durmuş P. and Yıldırım M., “Influence of interfacial layer thickness on frequency dependent dielectric properties and electrical conductivity in Al/Bi<sub>4</sub>Ti<sub>3</sub>O<sub>12</sub>/p-Si structures”, *Journal of Vacuum Science and Technology*, 32: 061512 (2014).
- [6] Reddy V. R., Manjunath V., Janardhanam V., Kil Y. H. and Choi C. J., “Electrical Properties and Current Transport Mechanisms of the Au/n-GaN Schottky Structure with Solution-Processed High-*k* BaTiO<sub>3</sub> Interlayer”, *Journal of Electronic Materials*, 43: 3499-3507 (2014).
- [7] Kaya A., Aliyaly S., Demirezen S., Balbaşı M., Yerişkin S. A. and Aytimur A., “The investigation of dielectric properties and ac conductivity of Au/GO-doped PrBaCoO nanoceramic/n-Si capacitors using impedance spectroscopy method”, *Ceramics International*, 42: 3322-3329, (2016).
- [8] Yerişkin S. A., Balbaşı M. and Tataroğlu A., “Frequency and voltage dependence of dielectric properties, complex electric modulus, and electrical conductivity in Au/7% graphene doped-PVA/n-Si (MPS) structures”, *Journal of Applied Polymer Science*, 133: 43827, (2016).
- [9] Chu L. K., Chiang T. H., Lin T. D., Lee Y. J., Chu R. L., Kwo J. and Hong M., “Ge metal-oxide-semiconductor devices with Al<sub>2</sub>O<sub>3</sub>/Ga<sub>2</sub>O<sub>3</sub>(Gd<sub>2</sub>O<sub>3</sub>) as gate dielectric”, *Microelectronic Engineering*, 91: 89-92 (2012).
- [10] Yıldırım M., “Current conduction and steady-state photoconductivity in photodiodes with bismuth titanate interlayer”, *Thin Solid Films*, 615: 300-304, (2016).
- [11] Jayalakshmi M. and Balasubramanian K., “Simple Capacitors to Supercapacitors - An Overview”, *International Journal of Electrochemical Science*, 3: 1196-1217, (2008).
- [12] Sze S. M., “Physics of Semiconductor Devices”, *Wiley*, New York, (1985).
- [13] Rhoderick E. H., “Metal-Semiconductor Contacts”, *Oxford University Press*, Oxford, (1978).
- [14] Altındal Ş., Kanbur H., Tataroğlu A. and Bülbül M. M., “The barrier height distribution in identically prepared Al/p-Si Schottky diodes with the native interfacial insulator layer (SiO<sub>2</sub>)”, *Physica B*, 399: 146-154, (2007).
- [15] Chattopadhyay P. and Raychaudhuri B., “Origin of the anomalous peak in the forward capacitance-voltage plot of a Schottky barrier diode”, *Solid-State Electronics*, 35: 875-878, (1992).
- [16] Lee, H. N., Kim, Y. T. and Choh, S. H. “Comparison of memory effect between YMnO<sub>3</sub> and SrBi<sub>2</sub>Ta<sub>2</sub>O<sub>9</sub> ferroelectric thin films deposited on Si substrates”, *Applied Physics Letters*, 76: 1066-1068, (2000).
- [17] Fujisaki Y., Kijima T. and Choh S. H., “High-performance metal-ferroelectric-insulator-semiconductor structures with a damage-free and hydrogen-free silicon-nitride buffer layer”, *Applied Physics Letters*, 78: 1285-1287, (2001).
- [18] Lee S. K., Kim Y. T., Kim S. I. and Lee C. E., “Effects of coercive voltage and charge injection on memory windows of metal-ferroelectric-semiconductor and metal-ferroelectric-insulator-semiconductor gate structures”, *Journal of Applied Physics*, 91: 9303-9307, (2002).
- [19] Altındal, Ş., Parlaktürk F., Tataroğlu A. and Bülbül M. M., “Temperature and frequency dependent dielectric properties of Au/Bi<sub>4</sub>Ti<sub>3</sub>O<sub>12</sub>/SiO<sub>2</sub>/Si (MFIS) structures”, *Journal of Optoelectronics and Advanced Materials*, 12: 2139-2144, (2010).
- [20] Card H. C. and Rhoderick E. H., “Studies of tunnel MOS diodes I. Interface effects in silicon Schottky diodes”, *Journal of Physics D: Applied Physics*, 4: 1589, (1971).
- [21] Nicollian E. H. and Brews J. R., “MOS Physics and Technology”, *Wiley*, New York, (1982).
- [22] Reddy M. S. P., Kang H. S., Lee J. H., Reddy V. R. and Jang J. S., “Electrical properties and the role of inhomogeneities at the polyvinyl alcohol/n-inp schottky barrier interface”, *Journal of Applied Polymer Science*, 131: 39773, (2014).
- [23] Reddy, V. R., Janardhanam, V., Leem, C. H. and Choi, C. J., “Electrical properties and the double Gaussian distribution of inhomogeneous barrier heights in Se/n-GaN Schottky barrier diode”, *Superlattices and Microstructures*, 67: 242-255, (2014).
- [24] Sharma B. L., “Metal-Semiconductor Schottky Barrier Junctions and Their Applications”, *Springer Science & Business Media*, (2013).
- [25] Fonash S. J., “A reevaluation of the meaning of capacitance plots for Schottky barrier type diodes”, *Journal of Applied Physics*, 54: 1966-1975, (1983).